Korean J. Chem. Eng., 36(5), 678-687 (2019)
DOI: 10.1007/s11814-019-0240-z

pISSN: 0256-1115
eISSN: 1975-7220

Preparation and characterization of a novel graphene/biochar composite and its application as an adsorbent for Cd removal from aqueous solution

Yan Li, Ningning Song†, and Kairong Wang†

Qingdao Engineering Research Center for Rural Environment/College of Resource and Environment, Qingdao Agricultural University, Qingdao, Shandong 266109, P. R. China
(*Received 1 November 2018 • accepted 11 February 2019*)

Abstract−A novel graphene/biochar composite (BG composite) was synthesized by mixing graphene (Gr) onto feedstock biomass followed by slow pyrolysis. The composite was then tested for its sorption capacity of Cd from aqueous solutions. Structure and morphology analysis showed that graphene was coated on the biochar surface, resulting in a larger surface area, more functional groups, greater thermal stability, and higher removal efficiency of Cd in comparison to unmodified biochar. The sorption capacity of the BG composite for Cd was 1.26-2.36 times that of biochar. A pseudo second-order model adequately simulated sorption kinetics. The sorption isotherms were simulated well by Langmuir models, and calculated maximum Cd adsorption capacities did not change significantly with increasing temperature. Thermodynamic parameters showed that the sorption process of Cd onto the BG composite was feasible and spontaneous. The results of the adsorption experiments, as well as the characteristics of biochar, demonstrate that the process of Cd adsorption on BG composites is mainly physical adsorption accompanied by other chemical adsorption phenomena, such as complexation and ion exchange. This study highlights the use of a BG composite as a multifunctional adsorbent for the efficient, economic, and environmentally friendly treatment of pollutants.

Keywords: Adsorption Capacity, Biochar, Cadmium, Graphene

INTRODUCTION

Cadmium (Cd) is an extremely toxic non-essential heavy metal that poses grave risks to public health and the environment [1]. The increasing industrial use of Cd and the massive exploitation of Cd-associated minerals has led to the continued increase of Cd-containing pollutants in the environment at an alarming rate. Cadmium causes serious damage to the bones and kidneys in humans and other living organisms via contaminated water and the food chain [2,3].

Traditional methods for removal of Cd, such as precipitation processes, electrochemical techniques, biological processes and adsorption approaches typically suffer from high costs, operational challenges, and produce toxic-sludge disposal problems [4-6]. In this context, the development of economically feasible and environment friendly methods for effective removal of Cd pollutants is of great importance.

Biochar is a carbonaceous residue produced by the thermal treatment of carbon-rich biomass at a limited concentration of oxygen [7,8]. It has lately been recognized as an effective adsorbent for removing a variety of contaminants from effluents, including heavy metals, polycyclic aromatic hydrocarbons (PAHs), organic pesticides and antibiotics [9-12]. However, the low sorption capacity of biochar prepared directly from biomass feedstock without pre- or post-treatments limits its application for removal of contaminants from industrial wastewater. Several approaches have been reported for the preparation of synthetic biochar-based composites by combining biochar with organic or inorganic materials via physicochemical methods for improvement of biochar properties, creation or incorporation of new structures and enhancement of the biochar sorption capacity [13].

Graphene is a single-atom-thick sheet of hexagonally arrayed sp^2-bonded carbon atoms. It has a large specific surface area (50-750 m^2/g) and has received much attention due to its remarkable properties [14]. Despite its excellent sorption ability, other potential risks such as poor water dispersion, along with high cost, are challenges to the application of graphene. While a great deal of progress has been in biochar research, studies into the use of graphene for modification of biochar to prepare modified materials and create novel composites are relatively lacking. Biochar/graphene composites (BG composites) combine the physiochemical properties of both biochar and graphene, resulting in improved biochar performance while maintaining a low cost of preparation [15,16]. However, research into the development of simple and convenient methods for the use of graphene for modifying biochar and its mechanism is rarely reported.

This study addresses these challenges by preparing and characterizing a BG composite of corn stalks and evaluating its Cd adsorption behavior. Sorption kinetics, sorption isotherms and influencing factors of the prepared BG composite were investigated to obtain a deep understanding of the sorption behavior. This work also aims to provide a scientific basis for practical application of the BG composite.

†To whom correspondence should be addressed.
E-mail: snn05@163.com, krwang1@163.com
Copyright by The Korean Institute of Chemical Engineers.

MATERIALS AND METHODS

1. Chemicals and Materials

All chemical reagents used in this study were of analytical grade. Graphene (diameter: 0.2-50 μm, thickness: 0.7-4 nm, carbon content: ≥97.9 wt%) was purchased from Shandong Jincheng Graphene Technology Co. Ltd. (Dongying, China). Corn stalks obtained from the local farmland, Qingdao, China, were air-dried and milled into powder (2 mm) as the feedstock biomass for biochar and BG composite production. The Cd solution was prepared by dissolving its sulfate salts (Sinopharm Chemical Reagent Co.) in a 0.01 M Na_2SO_4 solution. Deionized water was used for the preparation of solutions.

2. Preparation of Biochar and BG Composites

The biochar and BG composites used in this study were produced from corn stalks through a typical slow pyrolysis process. The pretreated corn stalk biomass was well mixed with graphene and placed in a sealed stainless-steel reactor tightly covered with a lid. The reactor was placed in a muffle furnace (Xianke, Inc., Longkou, Yantai, China) and heated at 100 °C for 1 h and at 350 °C for 3 h under O_2-limited conditions. Two types of BG composites were prepared by varying the mass ratios of graphene to corn stalks biomass (i.e., 1% and 5%). The original, biochar, and graphene/biochar composites were referred to as BC, BG1, and BG5, respectively.

3. Characterization of Biochar and BG Composites

The structure and surface morphologies of BC and BG composites were characterized by scanning electron microscopy (SEM; Zeiss EVO MA 10/LS 10, Carl Zeiss Co., Oberkochen, Germany). The surface area, pore volume, and pore size of the samples were determined using an automatic surface area analyzer (Quadrasorb SI, Quantachrome Co., Florida, USA). The elemental analysis for carbon (C), hydrogen (H), oxygen (O), nitrogen (N), and sulfur (S) involved using a CHN analyzer (vario EL cube, Elementar, Germany). The surface functional groups were observed on a Fourier transform infrared (FTIR) spectrometer (Nexus 670, Nicolet Co., Wisconsin, USA) by mixing the biochar sample with KBr. The scanning area was 4,000-500 cm^{-1}, and the resolution was 4 cm^{-1}. Details of the characterization of BC and BG composites are presented in Table 1.

4. Sorption Experiments

Adsorption kinetics and isotherms of Cd were obtained using a batch equilibration experiment. Adsorption kinetic experimental studies were performed with BC, BG1 and BG5 at a dosage of 1 g/L and an initial Cd concentration of 20 mg/L. The concentrations in a series of independent samples were shaken with the help of a rotary shaker (180 rpm) and measured from 0 to 180 min at room temperature (298.15 K). Isotherm experiments were performed for Cd at an initial concentration of 1-30 mg/L and the dosage of adsorbents was 1 g/L. The equilibrium time was measured after 180 min at 288.15 K, 298.15 K, 308.15 K and 318.15 K.

The effect of pH on adsorption of Cd by various adsorbents was investigated in the pH range 2.0-9.0. Each adsorbent (0.05 g) was added to a 50-mL solution with an initial Cd concentration of 20 mg/L and was reacted for 180 min at 298.15 K. To determine the effect of the adsorbent dosage, a 20 mg/L Cd aqueous solution was mixed with BC, BG1 or BG5 at dosages of 0.2, 1.0, 2.0, 3.0, 4.0 or 6.0 g/L. The experiment time was 180 min at room temperature.

Adsorption experiments used the corresponding initial concentration of heavy-metal solution as a control for deducing the effect of tube wall adsorption. After adsorption, the solution was centrifuged and filtered. The filtrate was collected, and the mass concentrations of Cd were analyzed by atomic absorption spectroscopy (AAS; Shimadzu AA-7000). The surface functional groups on biochar loaded with Cd were observed on an FTIR spectrometer. The "surface scanning" technique of the energy spectrometer (EDS) (FEI Inspect F50) was used to measure the main elements of the biochars.

5. Data Analysis

The concentration of adsorbed Cd at equilibrium, Q_e (mg/g), was calculated as follows:

$$Q_e=V(C_0-C_e)/m \quad (1)$$

where C_0 and C_e (mg/L) refer, respectively, to the original and equilibrium solute concentrations, V (L) is the solute volume, and m (g) indicates the amount of adsorbent.

Kinetic data were fitted with four classical kinetic models to reveal the adsorption mechanism. The governing equations of the mathematical models are as follows:

pseudo-first-order model (PF-order) [17]:

$$\ln (Q_e-Q_t)=\ln (Q_e-k_1t) \quad (2)$$

pseudo-second-order model (PS-order) [18]:

$$t/Q_t=1/(k_2\cdot Q_e^2)+t/Q_e \quad (3)$$

Table 1. Physical and chemical properties of Biochar and BG composite

Sorbents	S_{BET} (m^2/g)	Pore volume (cm^3/g)	Pore size (nm)	pH	Ash (%)	Yield (%)
BC	4.22±0.07	0.0091±0.001	8.81±0.02	7.70±0.02	16.6±0.14	32.2±1.30
BG1	7.02±0.01	0.0060±0.001	9.42±0.01	7.89±0.01	14.2±0.33	52.4±0.53
BG5	9.58±0.04	0.0149±0.002	8.76±0.05	8.68±0.01	23.1±0.42	42.5±1.22

	Content (%)					Atomic ratio		
	C	H	O	N	S	H/C	O/C	(O+N)/C
BC	68.13±0.09	4.18±0.06	18.44±0.31	2.17±0.09	0.12±0.01	0.74	0.20	0.23
BG1	54.18±0.09	4.24±0.17	23.89±0.35	2.32±0.09	0.16±0.01	0.94	0.33	0.37
BG5	58.19±0.13	3.40±0.21	18.58±0.17	2.46±0.01	0.19±0.02	0.70	0.24	0.28

$$h_0=k_2\cdot Q_e^2 \quad (4)$$

Intraparticle diffusion model (IPD) [19]: $Q_t=k_3\cdot t^{0.5}+c$ (5)

where Q_t (mg/g) represents the concentrations of Cd that the adsorbent removed at time t, k_1 (min^{-1}), k_2 (g/(mg·min)) and k_3 are the respective kinetic rate constants, c is the intercept of IPD, and t (min) is the adsorption time.

To estimate the capacity for and intensity of Cd sorption onto BC, Langmuir and Freundlich models were used to fit the experimental data of sorption isotherms.

Freundlich model: $Q_e=K_F\cdot C_e^n$ (6)

Langmuir model: $Q_e=(Q_m\cdot K_L\cdot C_e)/(1+K_L\cdot C_e)$ (7)

where C_e (mg/L) represents the equilibrium concentration of Cd, n is a parameter, and Q_m (mg/g) denotes the maximum adsorption capacity. K_F ((mg/g)/(mg/L)^n) and K_L (L/mg) represent the Freundlich and Langmuir constants, respectively.

The adsorption thermodynamic parameters Gibbs free energy (ΔG^0), entropy (ΔS^0) and enthalpy (ΔH^0) are calculated by the following equations:

$$\Delta G^0=-RT\ln K_L \quad (8)$$

$$\ln K_L=-\frac{\Delta H^0}{RT}+\frac{\Delta S^0}{R} \quad (9)$$

where ΔG^0 (J/mol) is the change in free energy, R (8.314 J/(mol·k)) is the gas constant, T (K) is the Kelvin temperature, K_L (L/mol) is the Langmuir isothermal model parameter, and the values of ΔH^0 and ΔS^0 are calculated from the slope and intercept of the plot of ΔG^0 and T.

RESULTS AND DISCUSSION

1. Characterization of Biochar and BG Composites

The structural morphology of biochar and BG composites was examined using SEM images (Fig. 1). BC were typically rough and porous in lamellar structure, whereas the layers of graphene on biochar surfaces bearing cavities could be clearly seen in BG1 and BG5. Graphene grew on the BC surface uniformly and smoothly by pyrolysis [20] without changing the original morphology of the biochar. With increasing graphene concentration, the finer attachments adhered to the surface of the biochar. The data presented in Table 1 shows that graphene wrinkles on the surface of the biochar could increase the surface area of the composites and favor deposition of environmental contaminants.

The selected physio-chemical properties of BC and BG composites are presented in Table 1. The properties of BG composites were improved compared to BC. All composites had pH values between 7.70 and 8.68. With increasing graphene content from 1% to 5%, the pH increased. The biochar yield reflected the degree of pyrolysis of the biomass feedstock. The 32.2% yield obtained for BC is similar to the solid products produced under hydrothermal carbonization processes reported by Xiao et al. [21]. The yield obtained for BG1 was 52.4%, which is higher than that obtained for BG5 (42.5%). While the ash content of BG1 was 14.2%, the ash content of BG5 was 23.1%, suggesting biochar yield decreases as the ash composition is enriched.

Surface area is an important indicator of adsorbent sorption ability [22]. The specific surface area was calculated by the Brunauer-Emmett-Teller (BET) model software (S_{BET}). The obtained S_{BET} values of BC (4.22 m^2/g), BG1 (7.02 m^2/g) and BG5 (9.58 m^2/g), lying within the range (1-50 m^2g^{-1}) of biochar produced from industrial organic waste such as eucalyptus sawdust [23], suggested that the addition of graphene provided additional surface area and some fine-pore structures for the BG composites [24]. However, the pore volume value of BG1 (0.0060 cm^3/g) was much lower than that of BC (0.0091 cm^3/g). These changes suggest the possible dispersion of graphene on the surfaces of biochar or stabilization within the pore structure, thereby increasing the surface area and reducing the pore volume [12]. The average pore sizes of BC, BG1 and BG5 were 8.81 nm, 9.42 nm and 8.76 nm, respectively, lying within 10 nm, which indicates that graphene did not alter the pore structure of biochar.

The elemental composition and atomic ratios of biochar and BG composites are shown in Table 1. As expected, the C value of BG1 (54.18%) and BG5 (58.19%) was less than that of BC (68.13%), while the nitrogen and sulfur content increased. The atomic H/C and O/C ratios are indexes of aromaticity and carbonization of biochar, respectively [25]. The atomic ratio of BG1 was 0.33 for O/C and 0.94 for H/C, significantly greater than BC (0.20 for O/C, 0.74 for H/C) and BG5 (0.24 for O/C, 0.70 for H/C), indicating that the biochar modified by 1% graphene has high hydrophobicity and more surface oxygenated functional groups through carboxylation or hydration. Similar phenomena were also observed

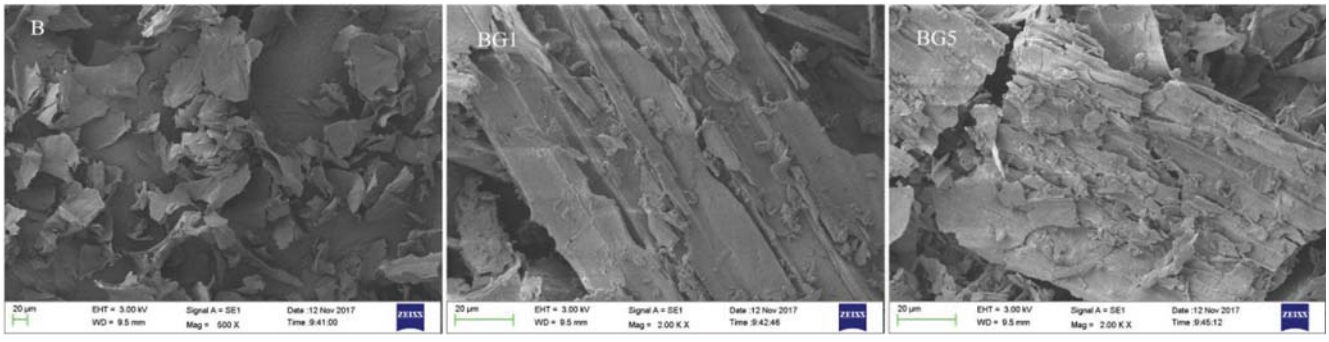

Fig. 1. Scanning electron microscope (SEM) images of BC, BG1 and BG5.

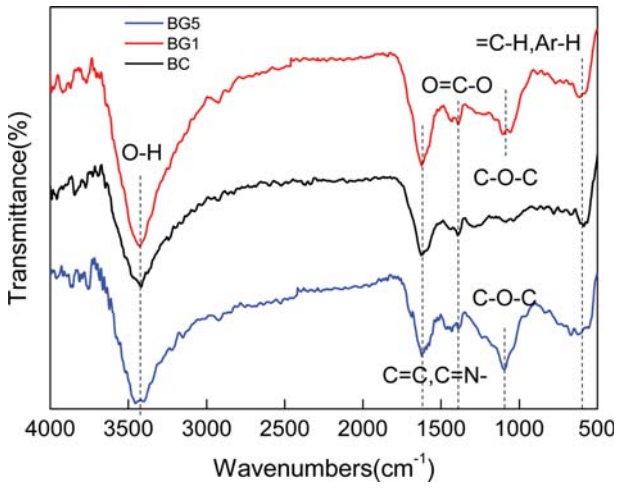

Fig. 2. FTIR image of BC, BG1 and BG5.

for the (O+N)/C atomic ratios.

The FTIR spectra for biochar and BG composites are shown in Fig. 2. The BC, GB1 and GB5 all showed a wide band at 3,300-3,500 cm^{-1}, which was attributed to hydroxyl (-OH) groups [25]. The bands from 1,600-1,595 cm^{-1} and 1,391 cm^{-1} can be attributed to the aromatic C=C and C=O groups of associated quinones, ketones, or both, and the carboxyl O=C-O stretching [25]. The bands at wavelengths 900-670 cm^{-1} were attributed to the vibration of alkyl olefin and aromatic C-H (=C-H, Ar-H), groups, indicating that the adsorbents have non-polar aliphatic functional groups and aromatic structure [26]. The peaks at 1,103 cm^{-1} for both BG1 and BG5 were assigned to alkoxy group C-O and stretching [27]. In addition, modification of biochar with graphene greatly increased the content of oxygen-containing groups of BG composites [28].

2. Adsorption Kinetics of Biochar and BG Composites

The adsorption kinetics of Cd on biochar and BG composites is presented in Fig. 3. Adsorption kinetics including film diffusion, intraparticular diffusion and adsorption on the surface of the adsorbent [29], which is an important aspect of process design and operational control, highlight the heterogeneous reaction and chemical adsorption mechanism [30]. PF-order, PS-order and IPD kinetic models were used to investigate adsorption kinetics in this study. The adsorption capacity of BG1 increased rapidly in the first 10 min and reached the adsorption equilibrium by approximately 30 min, while the adsorption capacity of BC and BG5 increased rapidly in the first 60 min and reached the adsorption equilibrium after approximately 120 min, suggesting that modification of BC with 1% graphene greatly increased the rate of the adsorption process. This is mainly because the dispersion of graphene-based adsorbents plays a significant role in the aqueous phase, and an appropriate content of graphene can accelerate the dispersion behavior of adsorbents in water [31].

The related kinetic parameters and coefficient of determination (R^2) values are listed in Table 2. For BG1 and BC, the PS-order model (R^2(BG1)=0.939, R^2(BC)=0.933) provided a better fit to kinetics than that of the PF-order model (R^2(BG1)=0.725, R^2(BC)=0.903) and IPD model (R^2(BG1)=0.612, R^2(BC)=0.890), as suggested by their higher correlation coefficients (R^2). The results sug-

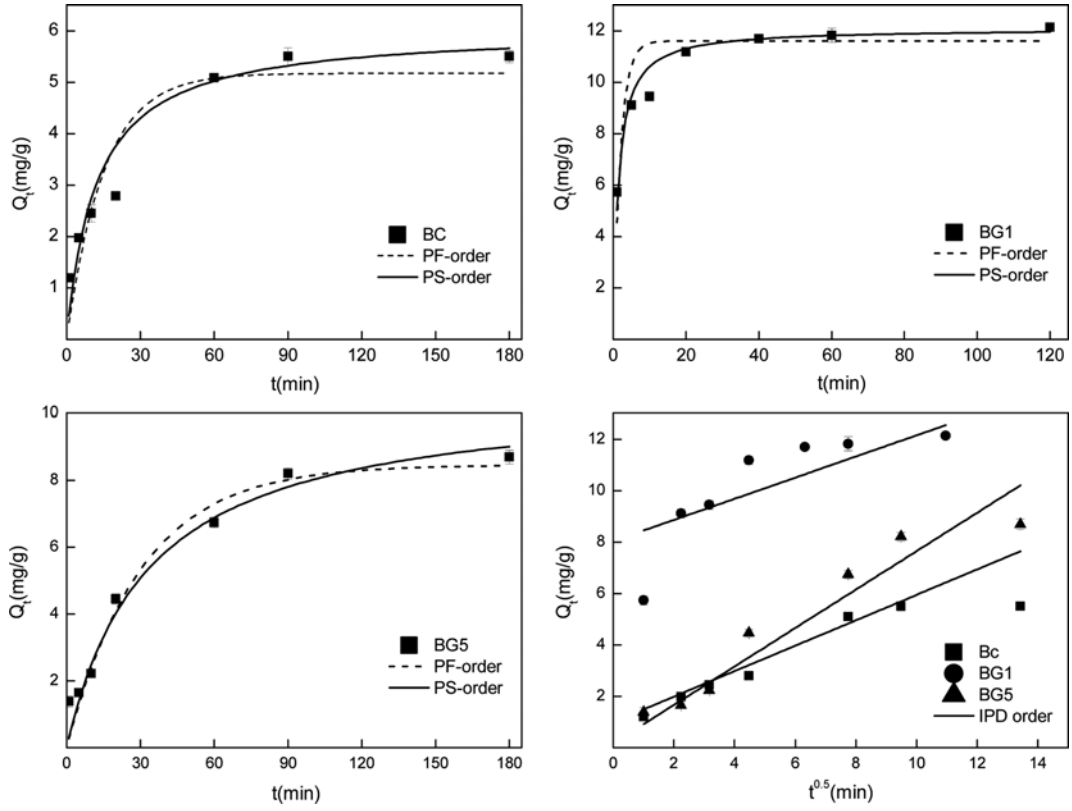

Fig. 3. Pseudo-first order (PF-order), pseudo-second order (PS-order) and IPD kinetics for Cd adsorption onto BC, BG1 and BG5.

Table 2. Constants and correlation coefficients of PF-order, PS-order and IPD kinetics models for Cd adsorption onto BC, BG1 and BG5

Sorbents	PF-order			PS-order				IPD		
	Q_e (mg/g)	k_1 (min^{-1})	R^2	Q_e (mg/g)	k_2 (mg/(g·min))	h_0 (mg/(g·min))	R^2	k_3	c	R^2
BC	5.174±0.29	0.066±0.020	0.903	6.037±0.45	0.013±0.005	0.474	0.933	0.497±0.07	0.998±0.48	0.890
BG1	11.60±0.41	0.497±0.170	0.725	11.09±0.23	0.058±0.011	7.133	0.939	0.411±0.13	8.039±1.03	0.612
BG5	8.455±0.57	0.033±0.005	0.964	10.664±0.91	0.003±0.001	0.341	0.966	0.747±0.09	0.169±0.46	0.919

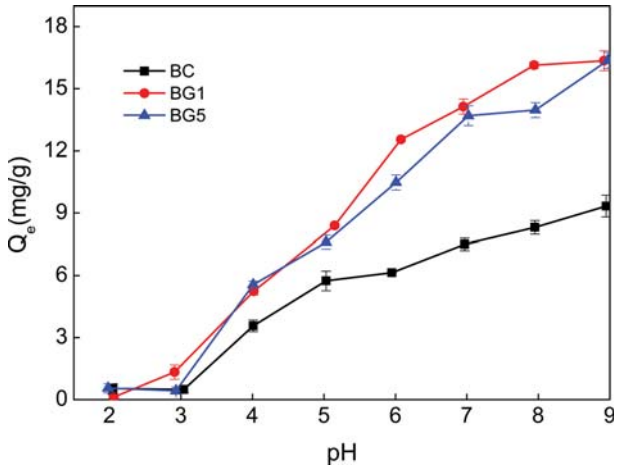

Fig. 4. Effect of pH for Cd adsorption capacities onto BC, BG1 and BG5.

gest that the sorption of Cd was predominantly a chemisorption process, involving electron sharing or electron transfer between the adsorbent and the adsorbate [13]. And the process rate of the first step is related to the availability of free-active sorption centers mainly on the biochar surface [32]. The adsorption rate (k_2) of BG1 (k_2=0.058) increased in comparison with that of BG5 (k_2=0.003), implying that a little content of graphene could cause a diffusive interaction over time to accelerate the initial Cd sorption. The h_0 is the initial adsorption rate of PS-order kinetic. The h_0 value of BG1 was 7.133 mg/(g·min), which was significantly greater than that of BG5 (0.341 mg/(g·min)), suggesting the BG1 has a higher initial sorption rate and the Cd molecules approach the biochar surface in a short time interval [33].

For BG5, both the PS-order model and IPD model accounted for the Cd adsorption kinetics. The Q_e calculated by the PS-order model was not much different from the experimental data, indicating that the kinetics of Cd adsorption onto BG5 was better in line with the PS-order model. Besides, the resulting straight lines of BG5 passed through the origin and therefore intraparticle diffusion was the rate-limiting step controlling the adsorption process [34].

3. The Effect of Solution pH on Cd Adsorption Capacity

The solution pH, an important parameter in sorption process optimization [29], affects both the surface charge and the dissolution of mineral components in the adsorbent, which in turn affects Cd adsorption [35]. The effects of pH on Cd removal by BC, BG1 and BG5 were studied. Fig. 5 reveals that the Cd adsorption capacity of BC, BG1 and BG5 increased with increasing initial solution pH. The adsorption capacity was steady in the pH range 2.0-3.0

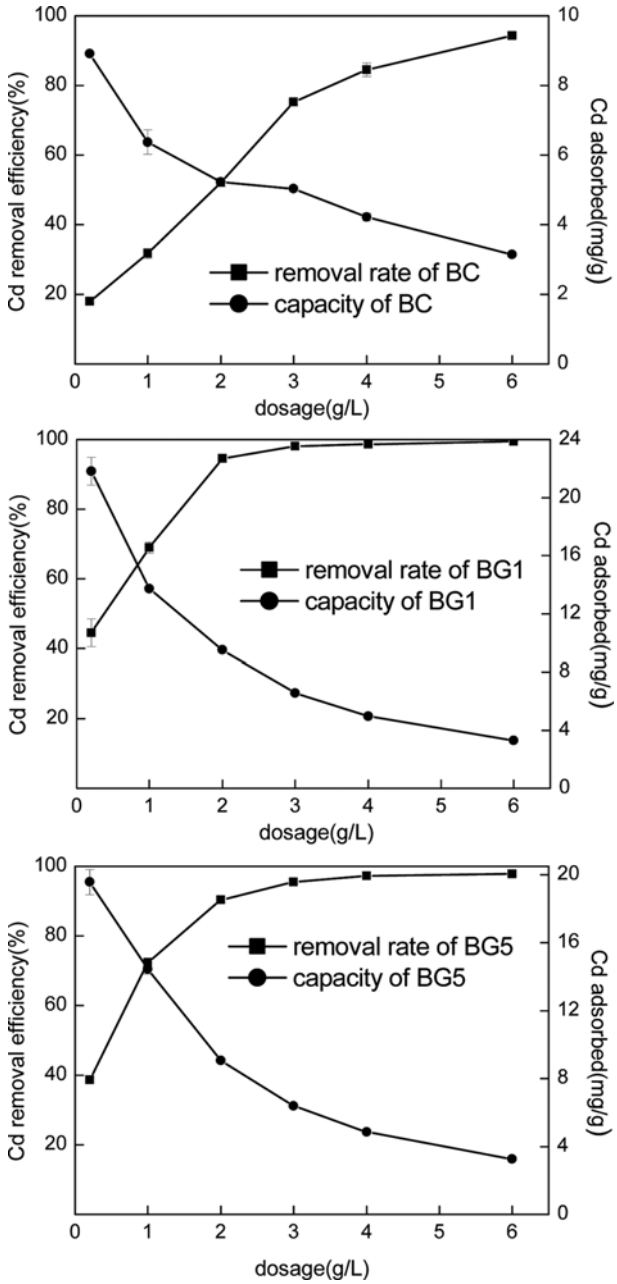

Fig. 5. Effect of BC, BG1 and BG5 dosage on the sorption of Cd.

and increased sharply when the initial solution pH ranged from 3.0 to 7.0, and increased slowly in the pH range 8.0-9.0. In the pH range 5.0-9.0, the adsorption capacity followed the order BG1> BG5>BC. According to earlier studies, at low pH, the positive charge

on the surface of biochar and the Cd in the solution were the repulsive actions of the same charge, which is not conducive to the biochar adsorption of Cd [36]. With increasing pH and the decrease of the hydrogen ions in the solution, the negative charge on the surface of the biochar increased, which is beneficial for hydrolysis because of the electronic structure of Cd [37,38]. Therefore, appropriately increasing the pH of the solution is beneficial for the adsorption of Cd.

4. Effect of Biochar and BG Composite Dosage on Cd Adsorption

The amount of the adsorbent is the most important factor influencing adsorption [39]. The effects of different amounts of BC, BG1 and BG5 on the sorption of Cd are summarized in Fig. 5. These findings are consistent with those previously reported by Elaigwu [40]. It can be seen that the adsorptive behavior of Cd on BG1 and BG5 was similar and the adsorption capacity of BG1 was higher than that of BG5. With an increase in the BG1 and BG5 dosages from 0.2 to 3 g/L, the Cd removal efficiency increased from 44.5% to 98.1% and from 38.6% to 95.5%, and subsequently became constant. These increases in the Cd removal efficiency with an increase in the adsorption dosage could be a result of the increase of the number of active sites [41,42]. Despite the increase in Cd removal efficiency with increasing adsorbent dosage, increasing the application rate of the adsorbent resulted in a decreased adsorption capacity of Cd, indicating that not all of the added sites were available for binding [43]. Overall, the optimized BG1 and BG5 dosage for Cd removal is 1-3 g/L. However, the increasing dosage of BC from 0.2 to 6 g/L enhanced Cd removal efficiency from 17.9% to 94.3%, indicating that 3-6 g/L of BC is optimum for Cd removal.

5. Adsorption Isotherms and Thermodynamics of Cd on Biochar and BG Composites

The adsorption isotherms of Cd onto biochar and BG composites described by Freundlich and Langmuir models at temperatures of 288.15 K, 298.15 K, 308.15 K and 318.15 K are shown in Fig. 4. The results indicate that the adsorption capacities of Gr, BC, BG1 and BG5 followed the order Gr<BC<BG5<BG1 at the four temperatures, suggesting that graphene did not directly increase the adsorption capacity of BG composites, but may have affected the carbonization process of BG composites, thereby increasing their adsorption capacity. The results of adsorption capacities were consistent with the results of the atomic H/C, O/C and (O+N)/C ratios of the adsorbents, implying that graphene may provide potential sites, thereby improving the adsorption capacity. A 1% content is the appropriate amount of addition, better than a 5% content. The Cd adsorption capacity of BG1 and BG5 increased with increasing adsorption temperature, indicating that increased temperature is a favorable factor in the adsorption process.

The related isotherm parameters and coefficient of determination (R^2) values of Freundlich and Langmuir models are summarized in Table 3. The non-linear exponent (n) values of all BC, BG1 and BG5 are less than 1.0, indicating that the biochar had a strong heterogeneity in the adsorption of Cd [44]. For both BG1 and BG5, the Langmuir model (R^2: 0.901-0.996) provided a better fit to isotherms than the Freundlich model (R^2: 0.802-0.951), identified by their higher correlation coefficients at these four temperatures, indicating that the Langmuir model was more suitable for the adsorption of Cd by BG1 and BG5 and that the type of adsorption was monolayer adsorption. The numerical values of K_L represent the stability of adsorbate and the adsorbent. The larger the value of K_L, the stronger the adsorption capacity, and the dimension of K_L was the inverse of the concentration. The values for BG1 are 2.622 and 1.653 at 288.15 K and 298.15 K, and 0.951 and 0.874 at 308.15 K and 318.15 K, respectively, which showed that the combination of adsorbent and Cd^{2+} was more stable than that at 308.15 K and 318.15 K, similar with that of BG5.

However, the Freundlich model was more suitable for the Cd adsorption of biochar BC. The K_f values were 3.242, 5.068, 7.232

Table 3. Constants and correlation coefficients of Freundlich and Langmuir models for Cd adsorption onto BC, BG1 and BG5

Sorbents	T (K)	Freundlich			Langmuir		
		K_F ((mg/g)/(mg/L)^n)	n	R^2	Q_m (mg/g)	K_L (L/mg)	R^2
Gr	288.15	0.326±0.025	0.599±0.026	0.995	3.790±0.338	0.055±0.009	0.991
	298.15	0.510±0.059	0.620±0.040	0.990	6.340±0.587	0.054±0.009	0.991
	308.15	0.512±0.079	0.703±0.053	0.987	10.571±0.463	0.033±0.007	0.992
	318.15	0.518±0.089	0.735±0.059	0.983	13.050±0.187	0.028±0.007	0.990
BC	288.15	3.221±0.106	0.345±0.015	0.995	8.887±0.792	0.471±0.253	0.903
	298.15	5.068±0.190	0.364±0.016	0.996	15.023±0.418	0.399±0.048	0.942
	308.15	7.232±0.391	0.337±0.025	0.988	18.630±0.231	0.516±0.047	0.912
	318.15	9.057±0.678	0.319±0.038	0.967	19.490±1.219	0.955±0.023	0.898
BG1	288.15	12.026±1.107	0.296±0.054	0.902	20.951±0.930	2.622±0.566	0.974
	298.15	11.148±0.145	0.330±0.016	0.837	22.179±0.767	1.653±0.295	0.924
	308.15	9.966±0.470	0.373±0.084	0.830	23.413±0.935	0.951±0.264	0.941
	318.15	10.907±1.519	0.416±0.091	0.844	26.372±1.895	0.874±0.297	0.924
BG5	288.15	9.137±1.121	0.281±0.061	0.859	17.792±0.310	1.561±0.125	0.996
	298.15	9.164±0.170	0.286±0.040	0.951	17.416±0.511	1.618±0.249	0.989
	308.15	6.733±0.037	0.502±0.081	0.922	25.583±0.759	0.354±0.103	0.960
	318.15	8.712±1.594	0.416±0.102	0.802	24.742±1.179	0.583±0.222	0.901

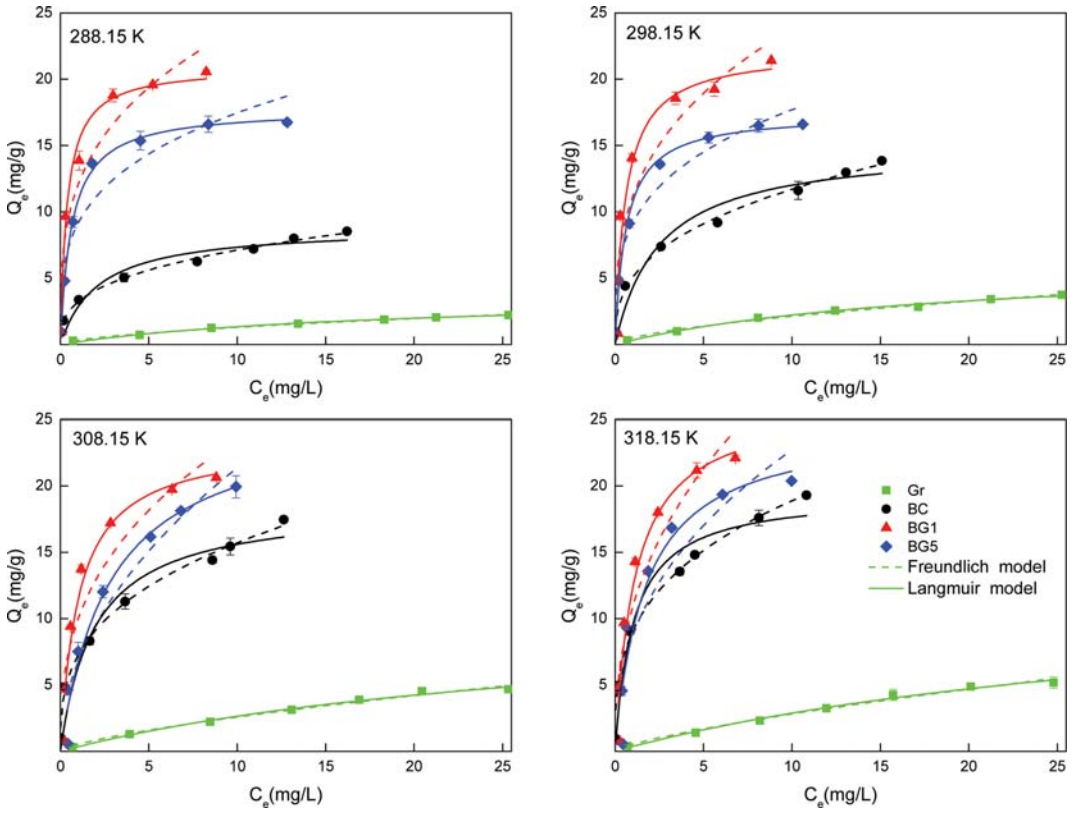

Fig. 6. Freundlich and Langmuir isotherms for Cd adsorption onto BC, BG1 and BG5 at a temperature of 288.15 K, 298.15 K, 308.15 K and 318.15 K.

and 9.057 at 288.15 K, 298.15 K, 308.15 K and 318.15 K, respectively, showing that K_F decreased with increasing temperature. When the n value was the same, the K_F value was comparable [45]. The results suggest that the investigated biochar and BG composites, especially BG1, are suitable for the removal of Cd from aqueous solutions.

To understand the inherent energetic changes in the adsorption process, it is important to evaluate thermodynamic parameters, such as ΔG^o, ΔH^o, and ΔS^o. Table 4 shows the results of thermodynamic parameters during adsorption. In this study, a negative value for ΔG^o showed that the Cd sorption onto Gr, BC and BG composites was spontaneous and feasible. For most of the studies, ΔG^o values were in the range of −30 to −10 kJ/mol, suggesting the participation of both physisorption and chemisorption in the adsorption process [31]. For BG1 and BG5, ΔG^o values were almost below −10 kJ/mol, indicating both physisorption and chemisorption in the sorption process. However, the absolute value of ΔG^0 changed slightly with the temperature increase from 288.15 K to 318.15 K, which showed that the Cd-biochar system was more stable with the biochar modified by graphene.

Table 4. Theemodynamic parameters for the sorption of Cd on BC, BG1 and BG5

Parameters	T (K)	Gr	BC	BG1	BG5
ΔG^0 (KJ/mol)	288.15	−4.36	−9.51	−13.62	−12.38
	298.15	−4.47	−9.43	−12.95	−12.90
	308.15	−3.36	−10.40	−11.97	−9.44
	318.15	−3.03	−12.37	−12.13	−11.06
ΔS^0 [J/(mol·K)]	-	−50.45	92.84	−55.53	−75.38
ΔH^0 (KJ/mol)	-	−19.10	17.72	−29.50	−34.30

In most studies, there is an enthalpy change in the range of 2-20 kJ/mol for physisorption, while it is 80-200 kJ/mol for chemisorption. The ΔH^o values of BG1 and BG5 were in the range of 20-80 kJ/mol, suggesting that there was both physisorption and chemisorption in the adsorption process of BG1 and BG5, which was consistent with the results of adsorption isotherms.

The value of ΔH^0 for BC was positive, indicating an increase in entropy. However, the value of ΔS^0 for BG1 and BG5 was negative, indicating that the randomness at the solid-solution interface during the adsorption of Cd on the graphene modified biochar was increased.

6. Possible Sorption Mechanism of Cd on BG Composites

The mechanism for Cd adsorption on biochar is very complicated. To probe the sorption mechanism between Cd and BG composites, FTIR and EDS were performed before and after sorption.

The FTIR spectra of the BG composites before and after Cd sorption were compared (Fig. 7). The peaks corresponding to the vibration of the hydroxyl-OH shifted from 3,426 cm^{-1} for BG1 to 3,407 cm^{-1} for Cd-laden BG1, and from 3,418 cm^{-1} for BG5 to 3,409 cm^{-1} for Cd-laden BG5. The vibration of C=C bond shifted from 1,624 cm^{-1} for BG1 to 1,614 cm^{-1} for Cd-laden BG1, and from 1,626 cm^{-1} for BG5 to 1,600 cm^{-1} for Cd-laden BG5. The peaks for the C-O bond at 1,103 cm^{-1} for BG1 and BG5 did not change

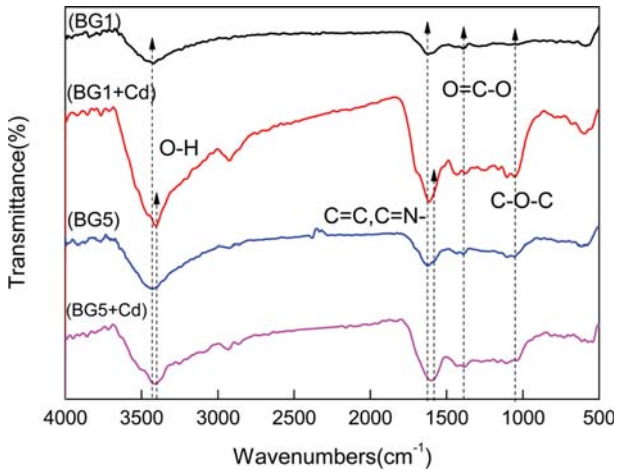

Fig. 7. Stacked FTIR spectra of BC, BG1 and BG5 before and after Cd adsorption.

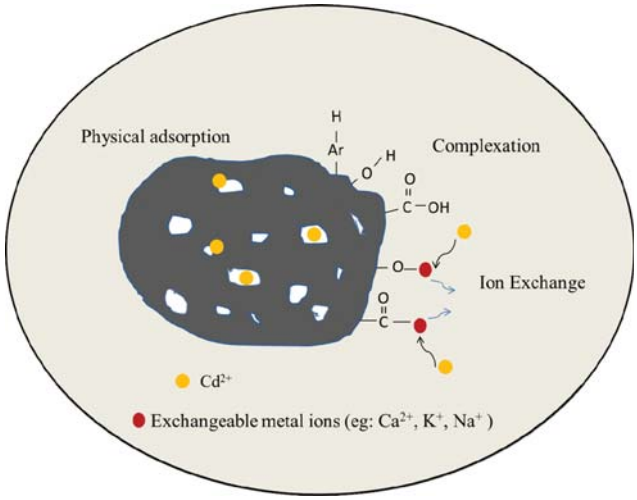

Fig. 9. Illustration of main mechanisms of Cd removal by BG composites.

after Cd sorption [46]. In addition, the stretching vibrations of the carboxyl O=C-O (BG1 1,391 cm^{-1}, BG5 1,392 cm^{-1}) disappeared after sorption for BG composites. The FTIR results indicated that oxygen-containing functional groups like C-O, -OH and O=C-O played an important role in the sorption of Cd.

EDS images are shown in Fig. 8. Many studies have reported that minerals or artificially derived minerals in nature can precipitate Cd on the mineral surface, thereby adsorbing Cd [47]. After sorption with Cd, the biochar meter in the energy spectrum scan image is rich in Cd element bright spots (Fig. 8(b) and Fig. 8(d)), which directly proves the adsorption of Cd by biochar.

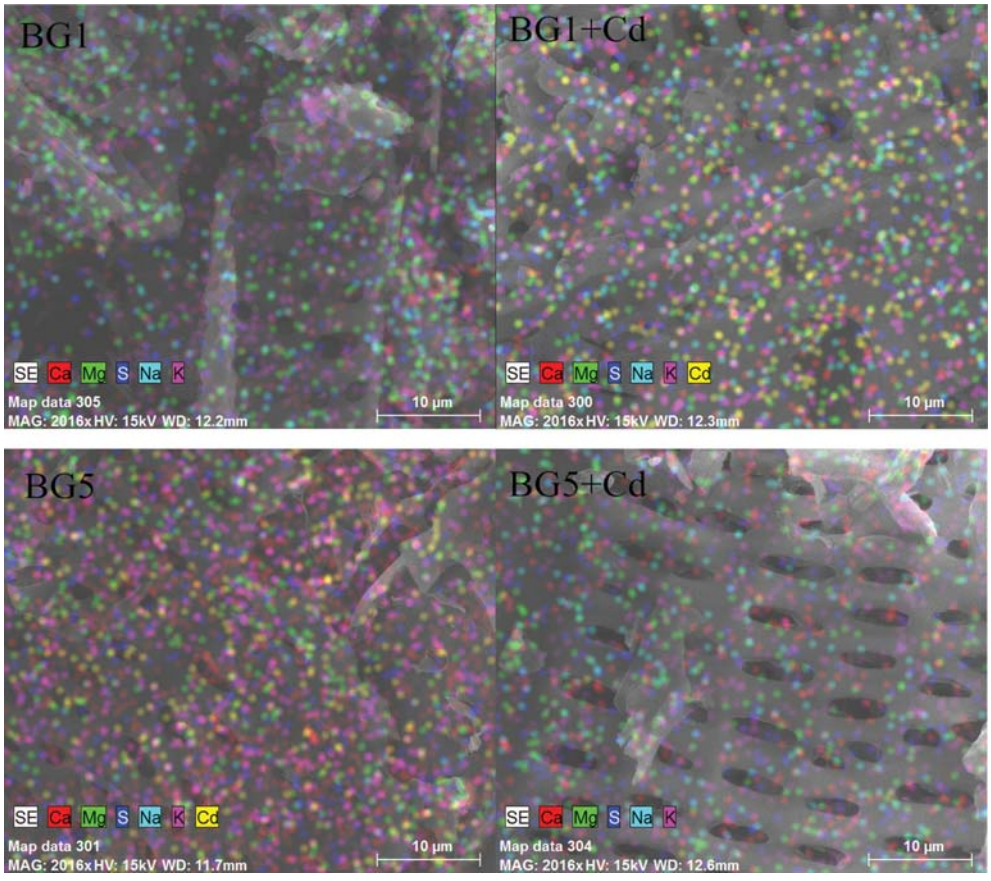

Fig. 8. Elemental mapping (EDS) of BG1 and BG5 before and after Cd adsorption.

The adsorption mechanism for Cd on biochar usually involves the comprehensive influence of several types of interactions, including complexation, ion exchange, and physical adsorption [48]. From the results of the kinetic, isotherm and thermodynamics experiments, we demonstrate that the process of adsorption of Cd on BG composites is mainly via physical adsorption accompanied by other chemical adsorption. The driving force of physical adsorption in porous adsorbent is mainly van der Waals force.

In summary, this study demonstrates that the mechanism of Cd^{2+} adsorption onto BG composites (Fig. 9) includes (1) physical adsorption (2) ion exchange with Ca^{2+}, Na^{+} and K^{+}, and (3) complexation of Cd^{2+} with hydroxyl functional groups.

CONCLUSIONS

BG composites were synthesized by mixing 1% and 5% graphene onto feedstock biomass followed by slow pyrolysis to improve the Cd adsorption capacity of biochar. The properties of BG composites showed drastic changes, such as surface area, pore volume, pore size and CHN elements in comparison to the original biochar counterpart due to the incorporation of graphene. Sorption capacity of the BG composites was much higher than BC, especially in the case of the 1% graphene/biochar composite. Results showed that Cd sorption onto BG composites was affected by pH of the solution and the dosage of adsorbents. The Cd adsorption kinetics and isotherms on BG composites were well-fitted to the pseudo-second-order model and the Langmuir isotherm, respectively. We demonstrated that the mechanism of Cd adsorption on BG composites was mainly physical adsorption accompanied by other chemical adsorption, such as cation exchange and complexation according to the results of the kinetic, isotherm and thermodynamics experiments. Further validation experiments with various actual industrial wastewater samples with a broader range of properties is necessary before BG composites can be used as effective adsorbents to remediate heavy metal contamination in wastewater.

ACKNOWLEDGEMENTS

This work was financially supported by National Natural Science Foundation of China (Grant No. 41701356 and 41701562), Research Foundation for Advanced Talents of Qingdao Agricultural University (Grant No. 6631115029 and 6631118002) and Graduate Student Innovation Program of Qingdao Agricultural University (Grant No. QYC201714).

REFERENCES

1. M. Idrees, S. Batool, Q. Hussain, H. Ullah, M. I. Alwabel, M. Ahmad and J. Kong, *Sep. Sci. Technol.*, **51**, 2307 (2016).
2. D. Mohan, C. U. Pittman, M. Bricka, F. Smith, B. Yancey, J. Mohammad, P. H. Steele, M. F. Alexandrefranco, V. Gómezserrano and H. Gong, *J. Colloid Interface Sci.*, **310**, 57 (2007).
3. P. Loganathan, S. Vigneswaran, J. Kandasamy and R. Naidu, *Critical Reviews in Environm. Sci. Technol.*, **42**, 489 (2012).
4. S. W. Won, P. Kotte, W. Wei, A. Lim and Y. S. Yun, *Bioresour. Technol.*, **160**, 203 (2014).
5. A. Moubarik and N. Grimi, *Food Res. Int.*, **73**, 169 (2015).
6. M. Bilal, J. A. Shah, T. Ashfaq, S. M. Gardazi, A. A. Tahir, A. Pervez, H. Haroon and Q. Mahmood, *J. Hazard. Mater.*, **263**, 322 (2013).
7. B. Chen, D. Zhou and L. Zhu, *Environ. Sci. Technol.*, **42**, 5137 (2008).
8. L. Beesley and M. Marmiroli, *Environ. Pollut.*, **159**, 474 (2011).
9. X. Cao, L. Ma, B. Gao and W. Harris, *Environ. Sci. Technol.*, **43**, 3285 (2009).
10. C. Zhang, G. Zeng, D. Huang, C. Lai, C. Huang, N. Li, P. Xu, M. Cheng, Y. Zhou and W. Tang, *Rsc. Advances*, **4**, 55511 (2014).
11. L. Qian and B. Chen, *Environ. Sci. Technol.*, **47**, 8759 (2013).
12. D. Huang, X. Wang, C. Zhang, G. Zeng, Z. Peng, J. Zhou, M. Cheng, R. Wang, Z. Hu and X. Qin, *Chemosphere*, **186**, 414 (2017).
13. M. Inyang, B. Gao, A. Zimmerman, M. Zhang and H. Chen, *Chem. Eng. J.*, **236**, 39 (2014).
14. M. Mehrali, S. T. Latibari, M. Mehrali, T. M. I. Mahlia, H. S. C. Metselaar, M. S. Naghavi, E. Sadeghinezhad and A. R. Akhiani, *Appl. Therm. Eng.*, **61**, 633 (2013).
15. M. Zhang, B. Gao, Y. Yao, Y. Xue and M. Inyang, *Sci. Total Environ.*, **435**, 567 (2012).
16. H. Wang, X. Yuan, Y. Wu, H. Huang, X. Peng, G. Zeng, H. Zhong, J. Liang and M. M. *Ren, Adv. Colloid Interface Sci.*, **195**, 19 (2013).
17. S. Lagergren, *Kungliga Svenska Vetenskapsakademiens Handlingar*, **24**, 1 (1898).
18. Y. S. Ho and G. Mckay, *Wat. Res.*, **34**, 735 (2000).
19. W. J. Weber and J. C. Morris, *Asce Sanitary Eng. Division J.*, **1**, 1 (1963).
20. J. Wang, Z. Chen and B. Chen, *Environ. Sci. Technol.*, **48**, 4817 (2014).
21. L. P. Xiao, Z. J. Shi, X. Feng and R. C. Sun, *Bioresour. Technol.*, **118**, 619 (2012).
22. J. Tang, H. Lv, Y. Gong and Y. Huang, *Bioresour. Technol.*, **196**, 355 (2015).
23. A. F. Martins, A. L. Cardoso, J. A. Stahl and J. Diniz, *Bioresour. Technol.*, **98**, 1095 (2007).
24. Y. Chun, G. Sheng, C. T. Chiou and B. Xing, *Environ. Sci. Technol.*, **38**, 4649 (2004).
25. M. Keiluweit, P. S. Nico, M. G. Johnson and M. Kleber, *Environ. Sci. Technol.*, **44**, 1247 (2010).
26. H. Zheng, Z. Wang, J. Zhao, S. Herbert and B. Xing, *Environ. Pollut.*, **181**, 60 (2013).
27. P. Devi and A. K. Saroha, *Bioresour. Technol.*, **169**, 525 (2014).
28. Y. Ren, N. Yan, J. Feng, J. Ma, Q. Wen, N. Li and Q. Dong, *Mater. Chem. Phys.*, **136**, 538 (2012).
29. D. Kołodyńska, R. Wnętrzak, J. J. Leahy, M. H. B. Hayes, W. Kwapiński and Z. Hubicki, *Chem. Eng. J.*, **197**, 295 (2012).
30. Y. Shen, X. Zhu and B. Chen, *J. Mater. Chem. A*, **4**, 12106 (2016).
31. N. K. Gupta and A. Gupta, *FlatChem*, **11**, 1 (2018).
32. V. Fristak, B. M. Richveisova, E. Viglasova, L. Duriska, M. Galambos, E. M. Jimenez, M. Pipiska and G. Soja, *J. Iran. Chem. Soc.*, **3**, 521 (2017).
33. G. Abdul, X. Zhu and B. Chen, *Chem. Eng. J.*, **319**, 9 (2017).
34. B. Wang, S. Y. Liu, F. Y. Li and Z. P. Fan, *Korean J. Chem. Eng.*, **34**, 1 (2016).
35. B. Li, L. Yang, C. Q. Wang, Q. P. Zhang, Q. C. Liu, Y. D. Li and R. Xiao, *Chemosphere*, **175**, 332 (2017).
36. G. Annadural, R. S. Juang and D. J. Lee, *Wat. Sci. Technol.*, **47**, 185

(2003).
37. V. Fristak, M. Pipiska, J. Lesny, G. Soja, W. Frieslhanl and A. Packova, *Environ. Monit. Assess.*, **187**, 1 (2015).
38. M. S. Polo and J. R. Utrilla, *Environ. Sci. Technol.*, **36**, 3850 (2002).
39. E. S. Z. El-Ashtoukhy, N. K. Amin and O. Abdelwahab, *Desalination*, **223**, 162 (2008).
40. S. E. Elaigwu, V. Rocher, G. Kyriakou and G. M. Greenway, *J. Ind. Eng. Chem.*, **20**, 3467 (2014).
41. A. K. Bhattacharya, S. N. Mandal and S. K. Das, *Chem. Eng. J.*, **123**, 43 (2006).
42. Q. Cheng, Q. Huang, S. Khan, Y. Liu, Z. Liao, G. Li and S. O. Yong, *Ecol. Eng.*, **87**, 240 (2016).
43. A. Usman, A. Sallam, Z. Ming, M. Vithanage, M. Ahmad, A. Al-Farraj, S. O. Yong, A. Abduljabbar and M. Al-Wabel, *Water Air Soil Poll.*, **227**, 449 (2016).
44. W. K. Kim, T. Shim, Y. S. Kim, S. Hyun, C. Ryu, Y. K. Park and J. Jung, *Bioresour. Technol.*, **138**, 266 (2013).
45. C. A. Coles and R. N. Yong, *Eng. Geol.*, **85**, 19 (2006).
46. M. Pipiska, B. M. Richveisova, V. Fristak, M. Hornik, L. S. Remenarova, G. Soja, J. Lesny and G. Soja, *J. Radioanal. Nucl. Chem.*, **311**, 85 (2017).
47. N. K. Gupta, A. Gupta, P. Ramteke, H. Sahoo and A. Sengupta, *J. Mol. Liq.*, **274**, 148 (2019).
48. H. Zheng, Z. Wang, X. Deng, J. Zhao, Y. Luo and J. Novak, *Bioresour. Technol.*, **130**, 463 (2013).
49. J. Deng, Y. Liu, S. Liu, G. Zeng, X. Tan, B. Huang, X. Tang, S. Wang, Q. Hua and Z. Yan, *J. Colloid Interface Sci.*, **506**, 355 (2017).